

On the Analysis of Expected Distance between Sensor Nodes and the Base Station in Randomly Deployed WSNs

Cüneyt Sevgi¹ and Syed Amjad Ali²

¹ Department of Information Technologies, Işık University, Istanbul, Turkey
csevgi@isikun.edu.tr

² Department of Computer Technologies and Information Systems, Bilkent University, Ankara, Turkey
syedalibilkent.edu.tr

Abstract. In this study, we focus on the analytical derivation of the expected distance between all sensor nodes and the base station (i.e., $E[d_{toBS}]$) in a randomly deployed WSN. Although similar derivations appear in the related literature, to the best of our knowledge, our derivation, which assumes a particular scenario, has not been formulated before. In this specific scenario, the sensing field is a square-shaped region and the base station is located at some arbitrary distance to one of the edges of the square. Having the knowledge of $E[d_{toBS}]$ value is important because $E[d_{toBS}]$ provides a network designer with the opportunity to make a decision on whether it is energy-efficient to perform clustering for WSN applications that aim to pursue the clustered architectures. Similarly, a network designer might make use of this expected value during the process of deciding on the modes of communications (i.e., multi-hop or direct communication) after comparing it with the maximum transmission ranges of devices. Last but not least, the use of our derivation is not limited to WSN domain. It can be also exploited in any domain when there is a need for a probabilistic approach to find the average distance between any given number of points which are all assumed to be randomly and uniformly located in any square-shaped region and at a specific point outside this region.

Keywords: Wireless sensor networks, Optimal cluster numbers, Energy efficiency, Random deployment, Base station location.

1 Introduction

A Wireless Sensor Network (WSN) is composed of a sheer number of *battery-powered* sensor nodes that communicate with each other through a *wireless* channel. Moreover, these nodes have *moderate* storage and application specific sensing capabilities in addition to their *limited* on-board processing power. Although WSNs suffer from scarcity of these resources, they offer promising potential to operate in unattended and harsh environments where the human-interacted or

the human-controlled monitoring schemes are risky, inefficient and sometimes infeasible.

In a typical WSN application, the main objective is to deploy a multitude sensor nodes working collaboratively in order to *cover* a given sensing field and to transfer (i.e., *connectivity*) the sensed data to the base station (BS). As such, coverage and connectivity are considered as two primary performance metrics and dominating factors that achieve the optimal use of an application's scarce resources for a given deployment scenario. The sensor nodes are deployed according to either scenario: the deterministic or the random deployment. In the deterministic deployment, the locations of the sensor nodes are known in priori. Conversely, in the random deployment, the locations of the sensor nodes are not deterministic as the term also indicates. The random deployment scenarios are used more frequently than their deterministic counterparts because the randomly deployed WSNs (RDWSNs) have higher potential to be devised in real-life scenarios especially when there is a need to monitor a physical phenomenon taking place in *hostile* and *inaccessible* environments.

Since there is a lack of prior knowledge about the locations of nodes in RDWSNs, the *connectivity* analysis is more stringent than the WSNs that adopt the deterministic deployment. In a deterministic scenario, the average distance between each node and its neighbors and similarly the average distance between each node and the BS are known in advance. However, in the random deployment scenarios, the above mentioned distances, which indeed affect the energy consumption and thus the lifetime of an application, are not known before the deployment. Therefore, it is really crucial for a network designer to estimate these distances as s/he needs to find out the modes of communication adopted by the network. These modes can be categorized as the *multi-hop* communication and the *direct* communication (a.k.a., single-hop). In a number of RDWSN applications, each sensor node is assumed to reach the BS within a single-hop. However, in those applications that adopt the direct communication, it is observed that a set of sensor nodes, which is far away from the BS, consumes a considerable amount of energy because it needs to perform long-haul transmissions. Therefore, those nodes, which are far from the BS, tend to die early and thus shorten the lifetime of the network. This is known as the *energy-hole problem*. To tackle the effects of this problem, the multi-hop communication is usually considered as more energy efficient than the direct communication. As such, in the process of making a decision on the communication modes, the network designer should need to compare the maximum transmission range with the expected value of the distance between each node and the BS ($E[d_{toBS}]$).

More importantly, $E[d_{toBS}]$ value also has an important role particularly for the *clustered* RDWSNs. In a clustering scheme, sensor nodes are basically *grouped* into clusters based on the proximity of the neighbouring nodes, the average distance to the BS, and energy levels, etc. to overcome some of the inherent challenges of WSNs. Clustering has been used as the most common technique due to its direct impact on the energy efficiency, network scalability and, more importantly, on the overall network lifetime. This is the reason why there are

numerous studies on this subject in the related literature. The reader is encouraged to refer to a recent and comprehensive survey [1] for an overview of different clustering schemes. In the studies analysing clustering schemes [2] and [3], it is revealed that $E[d_{toBS}]$ value is the key determinant to find out the optimum number of clusters (k_{opt}) that maximizes the lifetime in the clustered RDWSNs. A notable work in [3] proposes a number of closed-form expressions to identify k_{opt} . Amini et. al. provide a complete theoretical framework for characterization of k_{opt} with respect to a set of parameters of the system scenario listed as follows: the number of nodes to be deployed (N), the area of sensing field (A), and $E[d_{toBS}]$. The values for N and A are definitely known before the deployment. And the only thing the network designer needs to derive the $E[d_{toBS}]$ value to find k_{opt} value which maximizes the network lifetime. As such, the derivation of $E[d_{toBS}]$ becomes one of the central concerns in the clustered RDWSNs. In [3], the authors derive various expected values for the distance with numerous powers analytically and validate them through simulations. They mainly assume two *symmetric* sensing fields: a *disc* (with radius R) and a *square* (with side length M). By considering both a disc-shaped and a square-shaped sensing fields and a single BS, they find various $E[d_{toBS}]$ values for different powers (i.e., $E[d_{toBS}]$, $E[d_{toBS}^2]$, and $E[d_{toBS}^4]$). Amini et. al. analyze the $E[d_{toBS}]$ formulations by the varying locations of the BS as follows:

- The BS is located in the center
- The BS is located on the perimeter
- The BS is located outside the (on the axis of) sensing field

However, the case that gives $E[d_{toBS}]$ ($n = 1$) when the sensing field is square and the BS is located outside the field, is *missing* and therefore there is a gap to be filled. Herein, our main contribution is to articulate this gap by deriving $E[d_{toBS}]$ for this special case.

After outlining the main motivations of this study, we introduce a review of literature devoted to this topic to identify the reasons of clustering and the importance of optimum number of clusters in a clustered architecture. Following this review, Section 3 introduces the network model employed and the pertinent assumptions used throughout the paper. Section 4 illustrates our derivation of $E[d_{toBS}]$. Section 4 also includes the validation of our formulations. And the last section presents the conclusion of our study.

2 Related Work

Lifetime maximization is usually considered as one of the most important objectives in WSN applications. Lifetime maximization objective is mainly affected by the energy-hole problem. This problem is experienced when the nodes closer to the BS are usually required to forward a large amount of traffic for devices farther from the BS. The similar problem is also observed when a set of sensor nodes, which is far away from the BS, consumes a considerable amount of energy as it needs to perform long-haul transmissions. Therefore, these nodes tend to

die early which further results in energy holes. As far as the random deployment is concerned, the effects of energy-hole problem become even more serious. To minimize these effects, there are various studies which attack this problem. The most common technique to maximize lifetime in RDWSNs is to devise one clustering scheme or another. A clustering scheme typically groups sensor nodes into clusters to optimize the transmission distance for energy-efficiency and rotates the clusterheads for the evenly distribution of power loads. And the most widely-used and influential clustering scheme proposed is LEACH (Low-Energy Adaptive Clustering Hierarchy) [4].

LEACH mainly integrates the concept of energy-efficient cluster-based routing and medium access to prolong the system lifetime. It addresses the energy consumption minimization problems by making use of a distributed round-based algorithm. In each round of this distributed algorithm, it is expected that there are initially chosen number of clusters. And, after the competition of each round, clusterheads can be reelected periodically to balance the energy consumption. Thus, LEACH highly relies on the optimal number of clusters (k_{opt}) and in each round it is assumed that WSN consists of k_{opt} number of clusters. In [4], the authors describe whether there is an optimal tradeoff between the inter-cluster communication and the intra-cluster communication that balances energy consumption and they derive analytical expressions from simplifying and sound approximations. Analytical and simulation results are given to demonstrate the high performance of LEACH when compared with minimum transmission energy and static clustering. Thus, most of the studies dealing with clustering in WSN domain have been inspired by the study of LEACH. Thus, many variants of LEACH and the protocols that take the core idea from LEACH are systematically reviewed in [1].

HEED (Hybrid Energy-Efficient Distributed clustering) [5] is another protocol that aims to improve LEACH by periodically selecting clusterheads according to a hybrid of the node residual energy and a secondary parameter, such as node proximity to its neighbors or node degree.

Regardless of which clustering technique is employed or similarly which communication mode (i.e., multi-hop or single-hop) is exploited, a WSN application can only take the advantage of clustering if and only if the application is grouped with the optimum number of clusters. [3] analytically provides the optimal cluster size that minimizes the total energy expenditure in such networks, where all sensors communicate data through their elected clusterheads to the BS in a decentralized fashion. The analytical outcomes are given in the form of closed-form expressions for various widely-used network configurations. Extensive simulations are performed for the validation purposes when three cluster-based architectures namely LEACH, LEACH-Coverage, and DBS, are used.

One of the important concerns in the cluster-based architectures is the identification of k_{opt} . When portioning the WSN into clusters different from k_{opt} , the energy consumption of the WSN may become inefficient and it may degrade the network fast. Since the energy consumption of inter-cluster and intra-cluster transmissions of sensor nodes is a function of distance, k_{opt} depends on the

expected distance ($E[d_{toBS}^n]$) between the sensor nodes and the BS. There can be several scenarios where the BS will be positioned relative to the sensing field. A majority of these scenarios have been studied by [3] and $E[d_{toBS}^n]$ and thus k values are derived for $n=1$, $n=2$, and $n=4$ when the sensing field is a disc or a square. Authors addressed the problem of determining the k_{opt} of randomly deployed sensor nodes when the BS is located inside the field, on the perimeter and outside (on the axis of) the sensing field. It is observed that the derivation regarding one specific scenario is missing. Our contribution at this point is proposing the derivation of $E[d_{toBS}]$ of the missing scenario: when the sensing field is square and the BS is located outside the field.

3 Network Model

In this section, to facilitate the derivation of $E[d_{toBS}]$ expression, we describe the general system model and the pertinent assumptions used throughout the paper. As $E[d_{toBS}]$ value is mainly used to cluster a RDWSN with optimum number of clusters, herein we illustrate a sample RDWSN with the reduced number of devices before clustering in Figure 1(a) and after clustering in Figure 1(b). However, it should be noted once again that our derivations can also be exploited in any domain when there is a need for a probabilistic approach to find the average distance between any given number of points which are all assumed to be randomly and uniformly located in any square-shaped region and at a specific point outside this region.

For a RDWSN before clustering, let a square-shaped sensing field, with a surface area of M^2 , to be covered by N sensor nodes which are deployed randomly and uniformly over this field. Figure 1(a) simply illustrates this sample network with 22 devices before the cluster formation phase. After the calculation of k_{opt} value, suppose that 6 (say $k_{opt} = 6$) of the nodes switch to *clusterhead* role and 16 of the nodes keep on playing the ordinary sensor node role as can be seen in Figure 1(b).

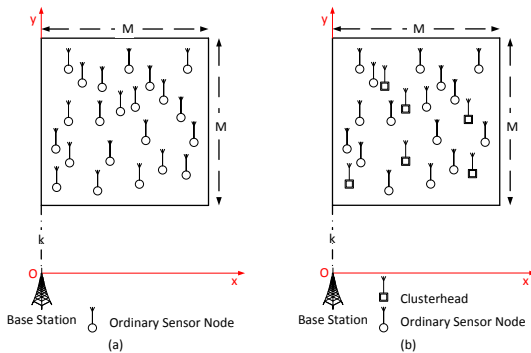


Fig. 1. A Sample Network Model (a) before clustering (b) after clustering

3.1 Assumptions

In this paper, all subsequent discussions are based on the following assumptions:

- The BS is assumed to be located at the *origin*. And the origin point is k units far away from the edge (on the axis symmetry) of the square-shaped sensing field as shown in Figure 1. The relative location of the BS is known in advance before the deployment.
- The BS is also assumed to have unlimited energy and thus there is no energy constraint associated with it. Moreover, all devices are assumed to be stationary and unattended.

4 Expected Distance between the Nodes and the BS

To derive $E[d_{toBS}]$ formulation, one should integrate the product of two functions over the entire sensing field. The first function determines the distance between a point and the BS. And the second function identifies the probability of a sensor node being at that specific point. First, we attempt to solve the problem by looking at double integrals in *Cartesian* Coordinates as shown in Figure 2(a). Recall that the infinitesimal area in the Cartesian Coordinates is $dA = dxdy$.

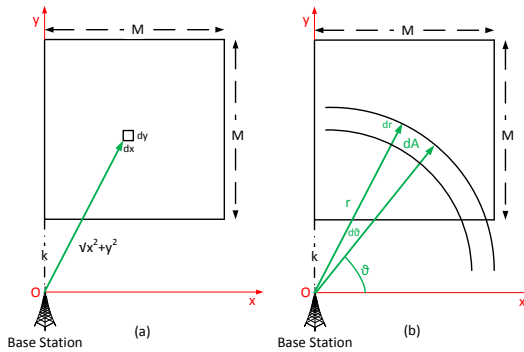


Fig. 2. Integration in the (a) Cartesian (b) Polar Coordinates

This is a rectangle with sides dx and dy . And, suppose that the probability of a sensor node being at point (x,y) , which is $\sqrt{x^2 + y^2}$ units away from the BS, is $p(x, y)$. Then, the integration to find $E[d_{toBS}]$ can be written as:

$$E[d_{toBS}] = \int \int p(x, y) \sqrt{x^2 + y^2} dxdy \tag{1}$$

Since, the probability of having a sensor node at each point inside the sensing field is identical¹, $p(x, y)$ is independent of x and y and is equal to $1/M^2$. By substituting $1/M^2$ value with $p(x, y)$ in Eqn. 1, we have:

¹ Due to the fact that the nodes are randomly and uniformly deployed and the sum of these probabilities is 1.

$$E[d_{toBS}] = 1/M^2 \int \int \sqrt{x^2 + y^2} dx dy \tag{2}$$

However, it is not trivial to find the integration in Eqn. 2 in the Cartesian Coordinates. Thus, we attempt to solve the same problem by using the *Polar* Coordinates and by integrating an infinitesimal ring-shaped element ($dA = r dr d\phi$). Before starting to integrate in the Polar Coordinates, recall that the probability of a sensor node being in the ring-shaped segment which is r radial distance from the BS is $p(r)$ as shown in Figure 2(b). Then, the integration to find $E[d_{toBS}]$ can be written in the Polar Coordinates as:

$$E[d_{toBS}] = \int \int p(r)r^2 dr d\theta \tag{3}$$

Similar to the probability value in the Cartesian Coordinates, $p(r)$ is equal to $1/M^2$. Therefore, we have:

$$E[d_{toBS}] = 1/M^2 \int \int r^2 dr d\theta \tag{4}$$

To be able to integrate $r^2 dr d\theta$ over the square-shaped sensing field, we need to consider two different regions with two different geometries. Thus, the sensing field is analyzed by dividing it into two separate regions as a triangle and a trapezoid as is shown in Figure 3(a) and (b) respectively.

4.1 Derivation of $E[d_{toBS-tri}]$ in a Triangle

Herein, we focus on the integration of $E[d_{toBS-tri}]$ over only the *triangular* region depicted in Figure 3(a). Boundary values for the integration are plugged in the Eqn. 4 when using the following trigonometric substitutions: $r_1 = A/\cos\theta$ and $r_2 = M/\cos\theta$

$$E[d_{toBS-tri}] = \frac{1}{M^2} \int_{\alpha_1}^{\alpha_2} \int_{A/\cos\theta}^{M/\cos\theta} r^2 dr d\theta \tag{5}$$

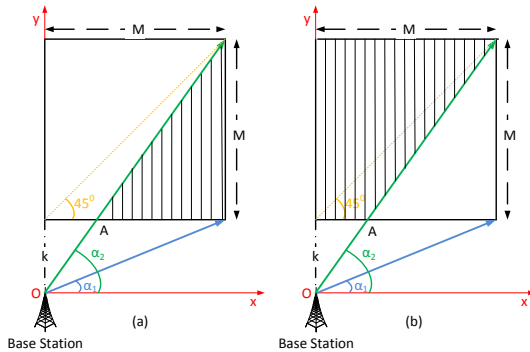


Fig. 3. (a) Shaded Triangular Region (b) Shaded Trapezoid Region

By using the similar triangles in Figure 3(a), we can denote the value of A in terms of k and M as:

$$\frac{k + M}{M} = \frac{k}{A} \Rightarrow A = \frac{k.M}{k + M} \tag{6}$$

Moreover, α_1 and α_2 can be expressed in terms of trigonometric identities as given in Eqn. 7 and 8 respectively.

$$\tan \alpha_1 = \frac{k}{M} \text{ and } \sec \alpha_1 = \frac{\sqrt{k^2 + M^2}}{M} \tag{7}$$

$$\tan \alpha_2 = \frac{k + M}{M} \text{ and } \sec \alpha_2 = \frac{\sqrt{(k + M)^2 + M^2}}{M} \tag{8}$$

Therefore, $E[d_{toBS-tri}]$ can be found as:

$$E[d_{toBS-tri}] = \frac{1}{M^2} \int_{\alpha_1}^{\alpha_2} \frac{r^3}{3} \Big|_{A/\cos\theta}^{M/\cos\theta} d\theta = \frac{M^3 - A^3}{3M^2} \int_{\alpha_1}^{\alpha_2} \frac{1}{\cos^3 \theta} d\theta \tag{9}$$

We replace the term A in Eqn. 9 with the substitute of A in Eqn. 6. Therefore, we have:

$$E[d_{toBS-tri}] = \frac{M}{3} \left(\frac{(k + M)^3 - k^3}{(k + M)^3} \right) \int_{\alpha_1}^{\alpha_2} \frac{1}{\cos^3 \theta} d\theta \tag{10}$$

In order to find the last term in Eqn. 10, we use Eqn. 11 which is from the table of integrals in [6]:

$$\int_{\alpha_1}^{\alpha_2} \frac{1}{\cos^3 \theta} d\theta = \frac{1}{2} [\tan \alpha_2 \sec \alpha_2 + \ln(\sec \alpha_2 + \tan \alpha_2)] - \frac{1}{2} [\tan \alpha_1 \sec \alpha_1 + \ln(\sec \alpha_1 + \tan \alpha_1)] \tag{11}$$

By replacing the trigonometric identities in Eqn. 7 and 8 with their substitute in Eqn. 11, we can find Eqn. 12. And finally, $E[d_{toBS-tri}]$ value for the triangular region is given in Eqn. 13.

$$\int_{\alpha_1}^{\alpha_2} \frac{1}{\cos^3 \theta} d\theta = \frac{1}{2} \left[\frac{(k + M)\sqrt{(k + M)^2 + M^2}}{M^2} + \ln \left(\frac{\sqrt{(k + M)^2 + M^2}}{M} + \frac{k + M}{M} \right) \right] - \frac{1}{2} \left[\frac{k\sqrt{k^2 + M^2}}{M^2} + \ln \left(\frac{\sqrt{k^2 + M^2}}{M} + \frac{k}{M} \right) \right] \tag{12}$$

$$E[d_{toBS-tri}] = \frac{M}{6} \left(\frac{(k+M)^3 - k^3}{(k+M)^3} \right) \left\{ \left[\frac{(k+M)\sqrt{(k+M)^2 + M^2}}{M^2} + \ln \left(\frac{\sqrt{(k+M)^2 + M^2}}{M} + \frac{k+M}{M} \right) \right] - \left[\frac{k\sqrt{k^2 + M^2}}{M^2} + \ln \left(\frac{\sqrt{k^2 + M^2}}{M} + \frac{k}{M} \right) \right] \right\} \quad (13)$$

4.2 Derivation of $E[d_{toBS-trap}]$ in a Trapezoid

Herein, we concentrate on the integration of $E[d_{toBS-trap}]$ over the *trapezoidal* region depicted in Figure 2(b). A trapezoidal region can be typically expressed by subtracting an area of a larger triangle from a smaller one. While the first term in the Eqn. 14 represents the larger triangle, the second one represents the smaller triangle.

$$E[d_{toBS-trap}] = \frac{1}{M^2} \left[\int_{\alpha_2}^{\frac{\pi}{2}} \int_0^{M+k/\sin\theta} r^2 dr d\theta - \int_{\alpha_2}^{\frac{\pi}{2}} \int_0^{A/\sin\theta} r^2 dr d\theta \right] \quad (14)$$

$$E[d_{toBS-trap}] = \frac{1}{M^2} \left[\int_{\alpha_2}^{\frac{\pi}{2}} \frac{r^3}{3} \Big|_0^{M+k/\sin\theta} d\theta - \int_{\alpha_2}^{\frac{\pi}{2}} \frac{r^3}{3} \Big|_0^{A/\sin\theta} d\theta \right] \quad (15)$$

$$E[d_{toBS-trap}] = \frac{1}{M^2} \left[\frac{(M+k)^3}{3} - \frac{A^3}{3} \right] \left[\int_{\alpha_2}^{\frac{\pi}{2}} \frac{1}{\sin^3\theta} d\theta \right] \quad (16)$$

Again by using the table of integrals in [6], the last term (B) in Eqn. 16 can be rewritten as:

$$\int_{\alpha_2}^{\frac{\pi}{2}} \frac{1}{\sin^3\theta} d\theta = \frac{1}{2} [-\cot\theta \csc\theta + \ln|\csc\theta - \cot\theta|] \Big|_{\alpha_2}^{\frac{\pi}{2}} = B \quad (17)$$

From Figure 3, we can easily find the following trigonometric identities:

$$\cot \frac{\pi}{2} = 0 \text{ and } \csc \frac{\pi}{2} = 1 \quad (18)$$

After $B = B' - B''$ substitution, we have:

$$B' = \frac{1}{2} \left[-\cot \frac{\pi}{2} \csc \frac{\pi}{2} + \ln \left| \csc \frac{\pi}{2} - \cot \frac{\pi}{2} \right| \right] = 0 \quad (19)$$

$$B'' = \frac{1}{2} [-\cot \alpha_2 \csc \alpha_2 + \ln |\csc \alpha_2 - \cot \alpha_2|] \quad (20)$$

$$B = \frac{1}{2} \left[\frac{M}{k+M} \frac{\sqrt{(k+M)^2 + M^2}}{k+M} \right] - \frac{1}{2} \ln \left| \frac{\sqrt{(k+M)^2 + M^2}}{k+M} - \frac{M}{k+M} \right| \quad (21)$$

$$E[d_{toBS-trap}] = \frac{1}{M^2} \left[\frac{(M+k)^3}{3} - \frac{A^3}{3} \right] B \quad (22)$$

By replacing the terms A and B in Eqn. 22 with their substitutes in Eqn. 6 and 21 respectively, we have the following:

$$E[d_{toBS-trap}] = \frac{1}{2M^2} \left[\frac{(M+k)^3}{3} - \frac{(\frac{k \cdot M}{k+M})^3}{3} \right] \left[\frac{M}{k+M} \frac{\sqrt{(k+M)^2 + M^2}}{k+M} - \ln \left| \frac{\sqrt{(k+M)^2 + M^2}}{k+M} - \frac{M}{k+M} \right| \right] \quad (23)$$

4.3 Derivation of $E[d_{toBS}]$ in a Square

Finally, to find $E[d_{toBS}]$, we add $E[d_{toBS-tri}]$ and $E[d_{toBS-trap}]$ expressions both for the triangle (Eqn. 13) and for the trapezoid (Eqn. 23). And, the formulation for our research problem is given in Eqn. 24

$$E[d_{toBS}] = \frac{M}{6} \left(\frac{(k+M)^3 - k^3}{(k+M)^3} \right) \left\{ \left[\frac{(k+M)\sqrt{(k+M)^2 + M^2}}{M^2} + \ln \left(\frac{\sqrt{(k+M)^2 + M^2}}{M} + \frac{k+M}{M} \right) \right] - \left[\frac{k\sqrt{k^2 + M^2}}{M^2} + \ln \left(\frac{\sqrt{k^2 + M^2}}{M} + \frac{k}{M} \right) \right] \right\} + \frac{1}{2M^2} \left[\frac{(M+k)^3}{3} - \frac{(\frac{k \cdot M}{k+M})^3}{3} \right] \left[\frac{M}{k+M} \frac{\sqrt{(k+M)^2 + M^2}}{k+M} - \ln \left| \frac{\sqrt{(k+M)^2 + M^2}}{k+M} - \frac{M}{k+M} \right| \right] \quad (24)$$

4.4 Validation

In order to validate our $E[d_{toBS}]$ formulation given in Eqn. 24, we compared it with Eqn. 42 in [3]. While the latter one assumes that the BS is located on the edge of the square-shaped sensing field, our derivation in Eqn. 24 assumes that the BS is arbitrarily located units outside the field. To adapt Eqn. 24 in this study to the one in [3], in other words, to move the BS from k units outside

the field to the edge of the sensing field, we assign $k = 0$ into Eqn. 24. After substituting 0 for k in Eqn. 24, we have the following expressions:

$$E[d_{toBS}] = \frac{M}{6} \left\{ \left[\sqrt{2} + \ln(\sqrt{2} + 1) \right] - [0 + \ln(1 + 0)] \right\} + \frac{1}{2M^2} \left[\frac{(M)^3}{3} \right] \left[\sqrt{2} - \ln|\sqrt{2} - 1| \right] \quad (25)$$

$$E[d_{toBS}] = \frac{M}{3} \left[\sqrt{2} + \ln(\sqrt{2} + 1) \right] \quad (26)$$

The fact that Eqn. 26 is exactly the same as the Eqn. 42 in [3] validates our finding.

5 Conclusion

We have formulated $E[d_{toBS}]$ when sensor nodes are deployed randomly and uniformly over a square-shaped sensing field and the BS is located outside the field. This expected value is required not only for the calculation of the optimum number of clusters in the clustered RDWSNs but also for the decision whether multi-hop or direct communication should be devised. One of the limitations of our derivation in this paper is that the BS is assumed to be located on the axis of (outside) the sensing field. Our future work will focus on this limitation and explore $E[d_{toBS}]$ when the BS is located at any *arbitrary* point *outside* the sensing field rather than at a specific point on the axis of the sensing field.

References

1. Tyagi, S., Kumar, N.: A systematic review on clustering and routing techniques based upon LEACH protocol for wireless sensor networks. *Journal of Network and Computer Applications* 36(2), 623–645 (2013)
2. Amini, N., Vahdatpour, A., Dabiri, F., Noshadi, H., Sarrafzadeh, M.: Joint consideration of energy-efficiency and coverage-preservation in microsensor networks. *Wireless Communications and Mobile Computing* 11(6), 707–722 (2011)
3. Amini, N., Vahdatpour, A., Xu, W., Gerla, M., Sarrafzadeh, M.: Cluster size optimization in sensor networks with decentralized cluster-based protocols. *Computer Communications* 35(2), 207–220 (2012)
4. Heinzelman, W., Chandrakasan, A., Balakrishnan, H.: An application-specific protocol architecture for wireless microsensor networks. *IEEE Transactions on Wireless Communications* 1(4), 660–670 (2002)
5. Younis, O., Fahmy, S.: HEED: a hybrid, energy-efficient, distributed clustering approach for ad hoc sensor networks. *IEEE Transactions on Mobile Computing* 3(4), 366–379 (2004)
6. Dwight, H.B., Hedrick, E.R.: *Tables of Integrals and Other Mathematical Data*, 3rd edn. The Macmillan Company (1956)